

# Producing Super-Hydrophobic Surfaces with Nano-Silica Spheres

Rob J. Klein\*, P. Maarten Biesheuvel\*\*, Ben C. Yu,\*\*\* Carl D. Meinhart\*\*\*\*,  
and Fred F. Lange

Materials Department  
University of California, Santa Barbara  
California, CA 93106

\* Chemical Engineering, UCSB

\*\* Now: Exploratory Research, Shell Global Solutions Int'l., Amsterdam

\*\*\* Now: Agilent Technologies Inc., Palo Alto, CA

\*\* \*\* Mechanical and Environmental Engineering, UCSB

## Abstract

Polycrystalline alumina substrates were dip-coated in dilute suspensions formed with dispersed, nano-silica particles. The fractional surface coverage of the alumina substrate was varied between 0.05 to 0.4 by changing concentration of particles in the silica slurry. After a heat treatment to partially sinter the particles to the surface, the surface was made hydrophobic by a reaction with a solution containing fluorosilane molecules. Wetting measurements showed that the contact angle between the surface and water droplets increased with decreasing area coverage of nano-silica spheres, consistent with a previous theory, modified here to include the pressure of the water droplet. The modification of the theory predicts that the super-hydrophobic effect disappears when the particles become too widely spaced, causing the pressure of the water droplet to spontaneously wet the substrate.

## 1 Introduction

For centuries, eastern religions have recognized the purity of the lotus leaf. Its purity is caused by its super-hydrophobic surface, which allows water drops to form nearly spherical balls that collect water-loving dust particles as they roll off with very little contact resistance. In 1997, biologists Barthlott and Neinhuis [1] showed that small, waxy bumps on the lotus leaf produced this super-hydrophobic effect.

Prior to the understanding this biological cleaning method, several physical scientists correlated surface roughness to increased hydrophobicity exemplified by the pioneering work of Cassie and Baxter [2] and Wenzel [3] in the early '40s.

More recently, Onda et al. [4] produced one of the first synthetic super-hydrophobic surfaces (wetting angles  $> 140^\circ$ ) by anodically oxidizing an aluminum surface and treating the oxidized surface with a fluorosilane. They suggested that the hydrophobicity was due to the fractal nature of the rough surface. Tadanaga et al. [5] produced a super-hydrophobic surface with a special heat-treatment of an aluminum oxide surface film formed by a chemical precursor method. When heat-treated, the aluminum oxide crystallized to form a topography that resembled tall hills and deep valleys. This special surface became super-hydrophobic after being coated with a monolayer of fluoroalkyltrichlorosilane molecules. Tadanaga et al. [5] were the first to recognize that the water only wetted the tops of the hills and that air must be trapped in the valleys. They modeled the textured surface as periodic flat plateaus and deep channels to hypothesize that the liquid would only wet the plateaus as shown in Fig. 1, while gas was trapped within the channels. Assuming that the liquid and gas would form a wetting angle of  $\theta$  and  $\theta_g$  with the solid, respectively, they related the area fraction of the surface (plateaus) wetted by the liquid,  $f$ , to the apparent contact angle,  $\theta^*$ , of a liquid drop by

$$\cos \theta^* = -1 + f(1 + \cos \theta) \quad (1)$$

which is valid for  $\frac{\theta}{2}$ . Bico et al [6], who derived the same relation using a free energy argument, verified this relation by texturing a surface with periodic, micron-size silica features (e.g., wells, plateaus and channels, flat mesas) produced on a substrate with a micro-molding technique. The textured surfaces were also treated with a monolayer of fluoroalkyltrichlorosilane molecules.

In the current work, we further explore the relation between the fraction of wetted surface and the apparent contact angle of a water drop using relatively rough, polycrystalline surfaces that are textured with nano- silica spheres. In addition, we modify the current theory to include the pressure exerted on the meniscus to show that the super-hydrophobic surface is best achieved with very small fraction of nano-particles.

## **2 Experimental**

The ‘as received’ silica slurry (Snowtex-OL, Nissan Chemicals, Tokyo, 20 wt%, particle size  $45 \pm 5$  nm, pH  $3 \pm 1$ ) was diluted with deionized water to concentrations as low as 0.025 wt%. The pH was adjusted to  $6.0 \pm 0.2$  with tetramethylammonium hydroxide (TMAOH) to produce a well-dispersed slurry. At pH 6, the silica particles were expected to be attractive to the alumina substrates. [7]

Polycrystalline alumina substrates (Superstrate 996, CoorsTek, Golden, Colorado, thickness 0.51mm, unpolished) were cut into 1x1 cm pieces. The substrates were cleaned by ultrasonication in acetone, then in a cleaning solution (90% of 98%  $H_2SO_4$ , 10% of 30%  $H_2O_2$ ), and finally in a 1% HF solution, after which they were rinsed in deionized water.

Different substrates were immersed into the different silica slurries for 20 min, and slowly removed and allowed to dry in a vertical position. The coatings produced with low concentration slurries were not visible to the unaided eye. Slurries containing  $> 0.5$  wt % of silica produced visible surface variations and were deemed too concentrated to produce macroscopically regular surface coverage on the alumina.

The coated substrates were heat treated to 400°C for 20 min to partially sinter the silica spheres to the alumina surface. After heating, the specimens were placed in deionized water for 15 minutes to ensure that the surfaces were sufficiently hydrated to allow a reaction with the fluoroalkyltrichlorosilanes [8].

To obtain a hydrophobic surface, the silica-coated alumina samples were dried and placed in a mixture of 0.4 mL fluoroalkyltrichlorosilane (1H,1H,2H,2H-perfluorodecyltrichlorosilane, Lancaster Synthesis, Windham, NH), 3 mL chloroform, and 30 mL hexadecane under an argon atmosphere for 12 hours [8], after which they were rinsed in chloroform. Contact angle measurements were made using a contact angle goniometer (NRL CA Goniometer, Ram-Hart, Mountain Lakes, NJ), with deionized water droplets of diameter 1.0 to 5.0 mm.

Images of the surface were obtained with a scanning electron microscope (JSM 6300FEG, JEOL). The area fraction of the silica spheres on the alumina substrates was determined by counting the number of silica spheres per unit area and multiplying this number by the cross-sectional area of an average silica sphere (diameter = 45nm). Silica spheres observed in deep crevices were omitted from the analysis.

### **3 Results**

Figures 1a,b,c illustrates the typical particle distribution on the polycrystalline alumina surfaces coated with slurries containing 0.05, 0.10, and 0.40 wt % silica respectively. One can observe that the spheres have a somewhat larger size distribution than reported by the manufacturer, and many of the spheres are agglomerated. Since the particles form well-dispersed slurries, it is assumed that the agglomerates are produced after dip-coating as the meniscus moves during evaporation. The micrographs also illustrate the alumina grains and the surface topography they form, namely, deep irregular channels and nearly flat tops. At low slurry concentrations, the silica spheres appear to only cover the raised portions of the grains, while at higher concentrations, the coverage becomes more irregular, with some areas exhibiting

full surface coverage. Figure 2 plots the fraction of area covered vs. the weight percent of silica spheres in the slurry used to dip-coat the substrate.

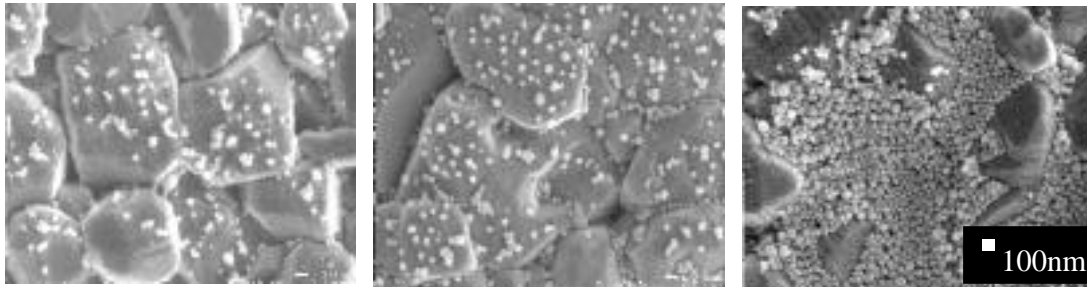


Figure 1. a), b), and c) are SEM micrographs illustrating the surface coverage of the of the 45 nm silica spheres on the polycrystalline alumina substrate produced by dip-coating with slurries containing 0.05, 0.10 and 0.40 wt % silica spheres.

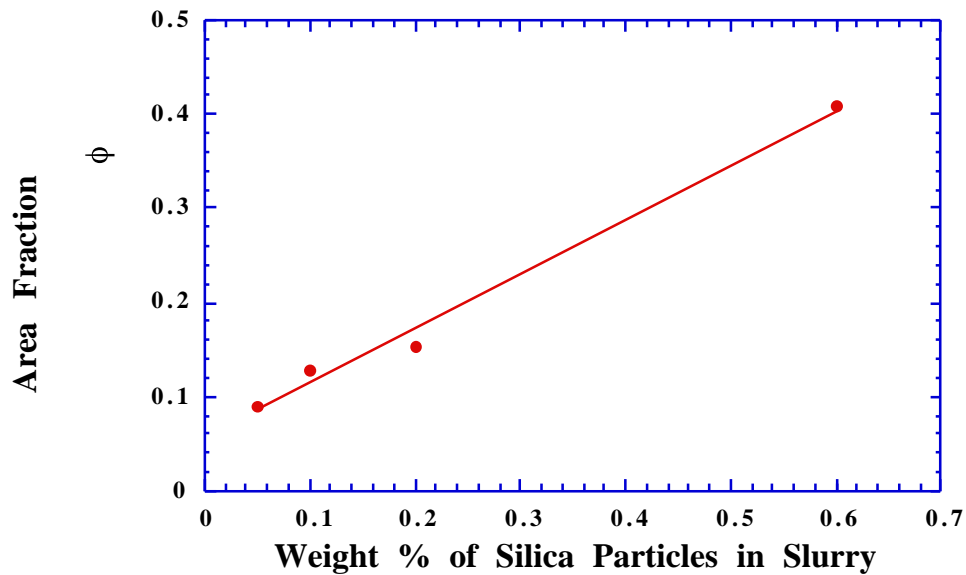


Figure 2 Experimental relation between wt % of silica spheres in the slurry vs fraction of surface area covered on polycrystalline alumina surface.

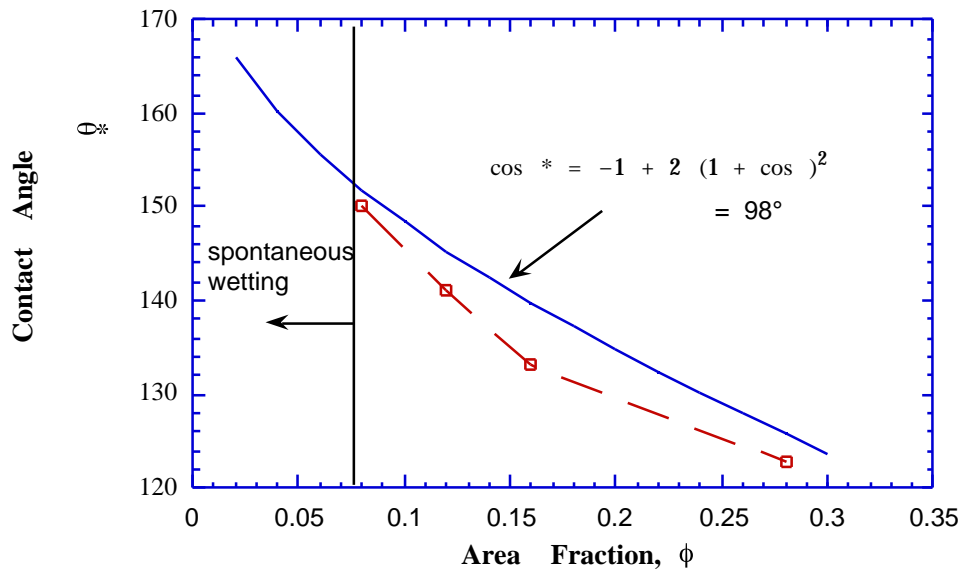


Figure 3. Measured contact angle  $\theta^*$  as a function of the area fraction,  $\phi$ , of the 45 nm silica spheres. The solid line shows the predicted contact angle, as per eq. (2), for  $\theta = 98^\circ$ . The vertical line shows the area fraction where the super-hydrophobic effect disappears.

Figure 3 plots the average contact angle,  $\theta^*$ , determined for each of the different surfaces against the fraction of area covered by the silica spheres. Although apparent contact angles of up to  $165^\circ$  were observed for area fractions less than what is shown in Fig. 3, these data were not reproducible, and thus, not shown.

#### 4 Discussion

The apparent contact angle for water drops on a hydrophilic surface textured with randomly distributed spheres increases with decreasing area fraction of spheres. This observation is consistent with that found by Bico et al. [6] who studied surfaces with three different textures with micron dimensions, namely, holes, plateaus & channels, and mesas. The Appendix treats the partial wetting of spheres that form a simple square lattice on the surface for

a liquid with a wetting angle,  $\theta > \pi/2$ . When the liquid/gas meniscus between the partially wetted spheres is flat (the pressure exerted by the water drop is neglected), the relation between the apparent contact angle  $\theta^*$ , the projected area fraction of the sphere on the substrate surface,  $\phi$ , and the wetting angle formed by a water drop on a flat surface,  $\theta$ , is given by

$$\cos \theta^* = -1 + 2 \phi (1 + \cos \theta)^2 \quad (2)$$

(Bico et al. [6] report a similar calculation, but miss the factor 2 in the second term.) Table I shows that when the experimental values of  $\theta^*$  and  $\phi$  are used in eq. (2) to determine the wetting angle of a flat surface. The predicted and experimental values of the wetting angle of a flat surface are in reasonable agreement. The calculated value of  $\theta$  for the polycrystalline alumina substrates assumes a flat surface, whereas, due to its polycrystalline nature, the surface (see Fig. 1) already has hills and valleys. This is consistent with the higher experimental value of  $\theta$  relative to the calculated value (105 ° vs. 94 °, respectively). For a flat silica surface  $\theta$  was found to be 98°, closer to the predicted values.

Table 1. Wetting angle,  $\theta$ , predicted using eq. (2) with experimentally determined variables ( $\theta^*$  and  $\phi$ ) for hydrophobic surfaces textured with silica spheres, compared to the experimental value of  $\theta$  determined on a flat surface.

Slurry, wt %	$\phi$	$\theta^*$ (degrees)	$\theta$ , predicted with eq. (2) (degrees)	$\theta$ , experimental (degrees)
0.05	0.085	150.1	96.6	105
0.10	0.120	141.0	92.1	105
0.20	0.173	133.1	92.5	105
0.40	0.285	122.9	96.0	105

The Appendix describes the effect of the pressure exerted by the water droplet on the meniscus. This pressure has two effects. First, because the meniscus is no longer flat, there is an

increase in both the wetted area of the solid, and the area of the liquid/gas interface. Second, and more important, the pressure can exceed a critical value where the meniscus either has a sufficient curvature to touch substrate between the spheres or produces an instability where the liquid spontaneously wets all surfaces.

Either event will eliminate the super-hydrophobic effect. As detailed in the Appendix, the critical pressure depends on the mass of the water droplet, the spacing and size of the spheres. For 45 nm silica spheres and size of the water drops used in the current experiments, the relations given in the Appendix suggest that the super-hydrophobic phenomena is expected to be lost for an area coverage  $\leq 0.001$ . This lower limit was calculated for a period, square array of spheres and is much smaller than obtained here  $\approx 0.08$ . It appears that the random spacing, or the fact that some areas are without spheres at lower area fractions, causes the critical area fraction to be larger than reported in the Appendix.

## **5 Conclusion**

Super-hydrophobic surfaces were obtained by simply dip-coating a substrate with a slurry containing nano-silica spheres, which adhered to substrate after a low temperature heat treatment. After reacting the surface with a fluoroalkyltrichlorosilane, the hydrophobicity increased with decreasing area fraction of spheres. These data support the theory of Tadanaga et al., [5] who hypothesized that a gas is trapped between the raised portions of the substrate to minimize the solid area in contact with the liquid. We have added to this theory to show that when the distance between the raised portions of the surface becomes too large, the mass of the droplet will cause spontaneous wetting to eliminate the super-hydrophobic effect.

## Appendix: Conditions for Spontaneous Wetting

We assume that the breakdown of the super hydrophobicity effect results from one of two phenomena. Both are caused by the finite weight of the droplet causing the meniscus to have a finite curvature. The first mechanism occurs when the pressure differential,  $P$ , across the meniscus becomes greater than a critical value,  $P_{cr}$ . When  $P > P_{cr}$ , the liquid will no longer wet the tops of the spheres, but the meniscus will spontaneously move to the substrate, thus wetting most of the spheres and the substrate. The second mechanism occurs when center of the curved meniscus touches the substrate, which will cause the shape of the meniscus to change and partially wet the substrate.

Let us begin by idealizing the randomly distributed particles, of diameter  $2r$ , as a periodic, square array with spacing  $2l$ , as shown in Fig. A-1. Relative to the atmospheric pressure, the liquid will exert a pressure forcing the meniscus between the spheres and thus forcing it to have a finite curvature. Fig. A-2 depicts the geometry of the liquid meniscus and its contact with the particles. The contact angle is denoted by  $\theta$ , while  $\alpha$  is angle between the tangent of the particle surface at the point of contact and the horizon, and  $\beta$  is the angle between the air/liquid interface and the horizon.

One can shown that

$$\beta = \alpha + \theta \quad (A-1)$$

is the projected area fraction of the spheres on the surface expressed as

$$f = \frac{r^2}{4l^2} \quad (A-2)$$

And  $d$ , the diameter of the wetted area of each sphere is given by

$$d = 2r \sin \theta \quad (A-3)$$

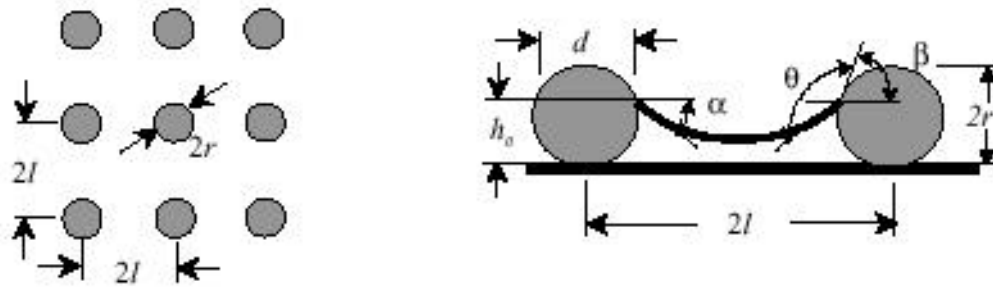


Fig. A-1. Top view of particles of Fig. A-2. Geometry of the meniscus wetting particles spaced diameter  $2r$ , placed in a square a distance  $2l$ , with a contact angle  $\alpha$ . The angle  $\beta$  defines the matrix of spacing  $2l$ . The tangent of the sphere with the horizon. The diameter of the wetted area is  $d$ .

As first taught by Laplace, for a given differential pressure,  $P$ , the equilibrium position of the meniscus can be determined by equating the vertical ( $y$  direction) force where the spheres support the meniscus to the opposing force exerted by the differential pressure on the meniscus. At equilibrium, the sum of these forces are

$$F_y = d \sin \alpha - P \frac{d^2}{4} = 0, \tag{A-4}$$

where  $\gamma$  is the surface energy per unit area of the meniscus.

Using the above equations, one can show that

$$P = - \frac{2 \gamma \sin \alpha \cos \beta}{r(1 - \sin^2 \alpha)}. \tag{A-5}$$

Equation (A-4) is equivalent to the Laplace equation, relating the differential pressure,  $P$ , across the meniscus to the geometry, defined by  $r$ ,  $\alpha$  and  $\beta$ , and to the specific surface energy ( $\gamma$ ) and wetting angle ( $\alpha$ ).

Inspection of eq. (A-4) shows that the maximum pressure the meniscus can sustain without being forced to the substrate occurs when  $\alpha = \pi/2$ . Thus, the largest and thus critical pressure the meniscus can support is given by

$$P_c = - \frac{2 \gamma \cos \beta}{r(1 - \sin^2 \alpha)} \text{ or } - \frac{2 \gamma \cos \beta}{r}, \text{ when } \alpha < 0.1. \tag{A-6}$$

Eq. (A-5) shows that, for a given size droplet, spontaneous wetting will occur below a critical volume fraction, i.e., the wetted particles become too widely spaced to support the meniscus. This relation also shows that the critical pressure for spontaneous wetting is inversely related to particle size.

The force exerted by a drop of diameter  $D$  is given by

$$F = \frac{\rho}{6} g D^3, \quad (\text{A-7})$$

where  $g$  is the acceleration of gravity and  $\rho$  is the density of the liquid. This force acts on a contact area  $(0.25 D^2 \sin^2 \theta^*)$  to produce a pressure on the meniscus that can be estimated, for  $\theta^* > 135^\circ$ , to be

$$P_d = \frac{2 \rho D}{3 \sin^2 \theta^*}, \quad (\text{A-8})$$

One determines the critical area fraction for spontaneous wetting by equating eqs. (A-6) and (A-8)

$$\phi_c = \frac{g D r}{3 \cos \theta^* \sin^2 \theta^*}. \quad (\text{A-9})$$

To test the second mechanism, the equilibrium shape of the meniscus was determined using the finite element package FEMLab™ (<http://www.comsol.com>). For the range of parameters of interest here, the results of the simulation showed that the contact line reaches the critical point on the particles (i.e.  $\theta = \pi/2$ ) before the center of the meniscus touches the substrate.

## Acknowledgment

Portions of this work were supported by NSF Award 0103514, CMS Division of Civil and Mechanical Systems Engineering. Rob Klein thanks the support of the Undergraduate Intern RISE Program at UCSB.

## References

- [1] W. Barthlott and C. Neinhuis, "Purity of the Sacred Lotus, or escape from contamination in biological surfaces," *Ann. Botany*, 79, 667 (1997).
- [2] A.B.D. Cassie and S. Baxter, "Wettability of Porous Surfaces," *Trans. Faraday Soc.*, 40 546 (1944).
- [3] R. Wenzel, "Surface roughness and contact angle," *J. Phys. Chem.*, 53, 1466 (1949).
- [4] T. Onda, S. Shibuichi, N. Satoh, K. Tsuji, "Super-water-repellent fractal surfaces," *Langmuir*, 12 [9] 2125-2127, (1996). [3] J Bico, C Marzolin, and D Quere. *Pearl drops*. *Europhys. Lett.*, 47 (1999) 220.
- [5] K. Tadanaga, N. Katata, and T. Minami, Super-Water-Repellent Al<sub>2</sub>O<sub>3</sub> Coating Films with High Transparency, *J. Am. Ceram. Soc.* 80 1040-1042 (1997).
- [6] J. Bico, C. Marzolin and D Quéré, "Pearl Drops," *Europhysics Lett.* 47 [2], 220-6 (1999).
- [7] M.L. Fisher, M. Colic, M.P. Rao, and F.F. Lange "Effect of Silica Nanoparticle Size on the Stability of Alumina/Silica Suspensions," *J. Am. Ceram. Soc.* (in press)
- [8] M.L. Hair, *Infrared Spectroscopy in Surface Chemistry*, p. 84-87, M. Dekker, New York (1967).